

Controlling Sonar Clutter via Higher-Order Statistics

R.C. Gauss and J.M. Fialkowski
Acoustics Division

Introduction: Active antisubmarine warfare sonar systems use acoustic sources and receivers coupled with signal processing to detect and classify undersea targets. The sources transmit broadband signals that propagate into, and interact with, the waveguide. The backscattered energy is received on high-resolution arrays and correlated (“match filtered”) with the transmitted signal, permitting a high degree of temporal and spatial localization in the search for potential targets. However, the limiting influence of clutter has long been recognized, with echoes from complex bathymetry, fish schools, and anthropogenic objects such as wrecks, capable of creating false targets that can both mask real targets and overload the sonar operator with false alarms.¹

To help reduce the false alarm rate, a variety of signal-processing strategies have been employed in analyzing the received data time series. In particular, statistical methods which provide measures of echo time-series characteristics, such as its spatial extent, rise time, and highlight structure, help to distinguish between real and false targets. NRL has been investigating higher-order statistical methods that allow extraction of even more information about the echoes, which in turn provide more reliable and robust clutter control.

Statistical Clutter Modeling: At the heart of statistical clutter modeling is a probability density function (PDF) of the matched-filter time series. Within each analysis window, the normalized time series data are histogrammed according to amplitude level. Clutter is defined as target-like echoes that result in false alarms (threshold exceedances) at the detector stage of the data processing. While background noise typically generates Rayleigh PDFs, clutter generates non-Rayleigh PDFs (Fig. 1(a)), which result in an increased probability of false alarm (PFA). Accordingly, from a sonar-performance perspective, characterizing and controlling the tails of these data distributions is paramount. While many PDFs have been explored over the years, very few have a physical basis. NRL has recently developed the physics-based Poisson-Rayleigh (P-R) PDF that models data amplitudes as a joint process arising from two statistically independent mechanisms, namely returns from a continuous background and a set of acoustically strong discrete scatterers.² Its key parameters are α , which represents the effective number of discrete scatterers, and ρ_D^2 , their relative strength.

Higher-order statistics (HOS) refer to functions involving the third or higher sample moments; for example, skewness and kurtosis are respectively the 3rd and 4th normalized moments. One way to assess a PDF model’s generality or narrowness in representing higher-order moments and matching data is to examine how it depends on skewness γ_3 and kurtosis γ_4 , as they represent scale-invariant measures of departure from normality: skewness represents PDF asymmetry and kurtosis PDF shape. By its capability to represent a much wider range of (γ_3, γ_4) values (Fig. 1(b)), the multiparameter P-R model has a clear advantage in describing data distributions (Fig. 1(a)) over conventional single-parameter models (such as the lognormal). Another advantage of the P-R model is that its parameters can be efficiently estimated from the data via the 2nd, 4th, and 6th moment equations of the P-R distribution.

Clutter Control: NRL has developed a sonar clutter-control method based on the P-R PDF model that leverages the P-R parameters’ relatability to scatterer attributes (density, spatial dispersion, and relative strength).³ The model parameters are first estimated from data prior to thresholding within analysis windows of fixed time duration (range extent). Next, these quantities are mapped to range-bearing or latitude-longitude cells to form distributions of parameter values associated with echo returns on a sonar display. Classification features are then derived from parameter distribution statistics associated with each data cell. Lastly, the relative values of these features are used to classify echo returns based on scatterer characteristics, thereby providing a physical basis for distinguishing real from false targets.

Results: The clutter-control method has been demonstrated using broadband data collected with coherent sources and towed horizontal receiver arrays in both a geologically complex environment, the Malta Plateau (south of Sicily) during the Boundary 2004 (B2004) experiment (Fig. 2(a)), and a biologically complex Gulf of Maine environment during a 2011 experiment (GOM2011). During B2004, additional sources of echoes were of anthropogenic origin (an offshore oil platform, a water-column-spanning pipe used to moor its tending tanker, and a passive reflector). Due to their spatial compactness in range, the pipe and passive reflector serve as surrogate target objects.

Figures 2 and 3 demonstrate on real-world data the potential of our clutter classification technique for improved rejection of clutter relative to target-like objects. Figure 2 shows how application of our method effectively eliminates the pervasive bottom clutter associated with the Ragusa ridge (Fig. 2(b)), while

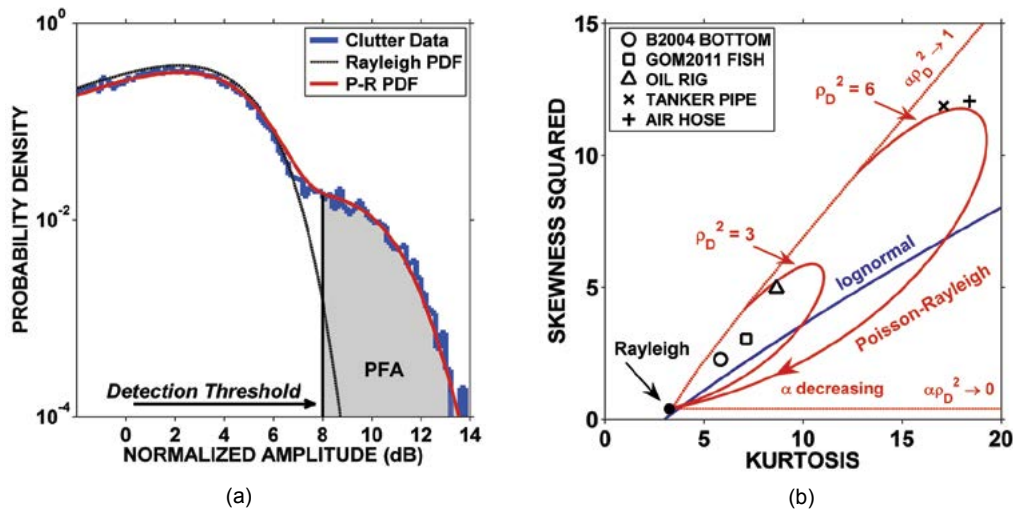


FIGURE 1
 (a) PDF of sonar data, and (b) distribution of data and model values in the (γ_4, γ_3^2) plane.

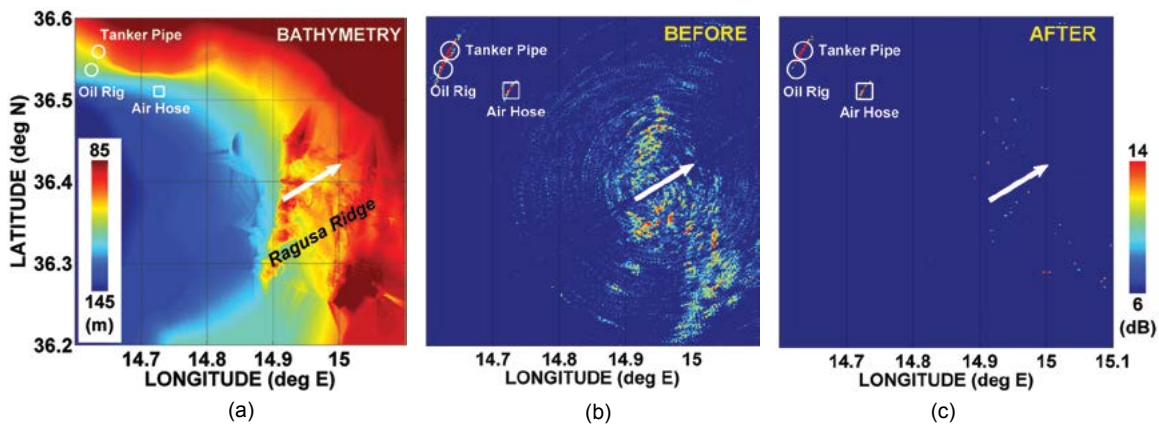


FIGURE 2
 (a) Malta Plateau bathymetry and active sonar track (white arrow), (b) georeferenced clutter and target-like echoes, and (c) reduction in clutter after applying our classification method.

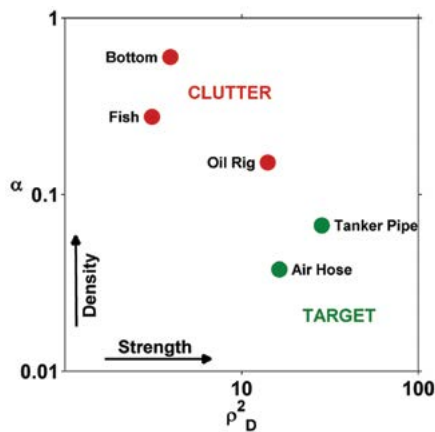


FIGURE 3
 Classification of echoes by their derived P-R parameter values.

retaining echoes from the more target-like objects (Fig. 2(c)). Figure 3 further shows how our P-R parameter

estimates can separate different classes of echoes. Significantly, the data results additionally suggest that in contrast to current methods, this new moment-based technique can provide feature information that is largely independent of an echo's signal-to-noise ratio (SNR) — this could allow lowering the detection threshold, and so enhance detection of low-SNR targets.³ Assessing the general utility of this method and optimizing performance in terms of environmental and system variables remains the focus of current work.

[Sponsored by the NRL Base Program (CNR funded)]

References

- ¹ R.C. Gauss, "Characterizing and Controlling Reverberation and Clutter," Ch. 12 in *Important Elements in: Geoacoustic Inversion, Signal Processing, and Reverberation in Underwater Acoustics*, ed. A. Tolstoy (Research Signpost, India, 2008), pp. 327–370.
- ² J.M. Fialkowski, R.C. Gauss, and D.M. Drumheller, "Measurements and Modeling of Low-Frequency Near-Surface Scattering Statistics," *IEEE J. Ocean. Eng.* **29**, 197–214 (2004).

Transition and Optimization of a Fast Broadband Pulse Propagation Algorithm for Fleet Use

R.A. Zingarelli
Acoustics Division

Introduction: An algorithm to minimize the number of frequency-domain model runs needed for Fourier synthesis of broadband time-domain pulses, developed earlier under NRL 6.2 Base Funding,¹ has been transitioned to Fleet use as part of the Navy Standard Parabolic Equation model (NSPE)² package. The method is based on observed regularities in acoustic phase and magnitude variation with frequency, in single-frequency model results. These regularities allow many of the model runs, which would normally be required by the Nyquist sampling condition, to be omitted and later filled in through phase and magnitude interpolation. In transitioning this algorithm to automated operational use, further optimizations were combined and exploited to give even greater computational efficiencies. In operational applications, this method allows a roughly 20-fold speedup over conventional Fourier synthesis techniques, while remaining robust enough for Fleet use. In a limited number of benchmark test cases, up to 650-fold speedups have been achieved.

Method: Fourier synthesis of time-domain (TD) results from a set of single-frequency results of continuous-wave (CW) modeling is a standard numerical analysis technique.³ Parabolic equation (PE) based CW acoustic models, such as the NSPE, generate complex output field values at each computational grid point. Examination of complex PE results at a single receiver location show that the phase and magnitude vary with significant regularity, as shown in Fig. 4. The phase varies almost linearly with frequency, wrapping back whenever its usual $-\pi$ to π bounds are exceeded, while the magnitude is a smoothly varying simple curve. Using the average slope near the center frequency of the TD pulse being propagated, the phases can be unwrapped. Intermediate phase and magnitude values can then be linearly interpolated, either to reduce the frequency spacing and thus increase the time window duration, or — as done here — to provide a frequency skipping optimization to eliminate a large number of CW model runs.

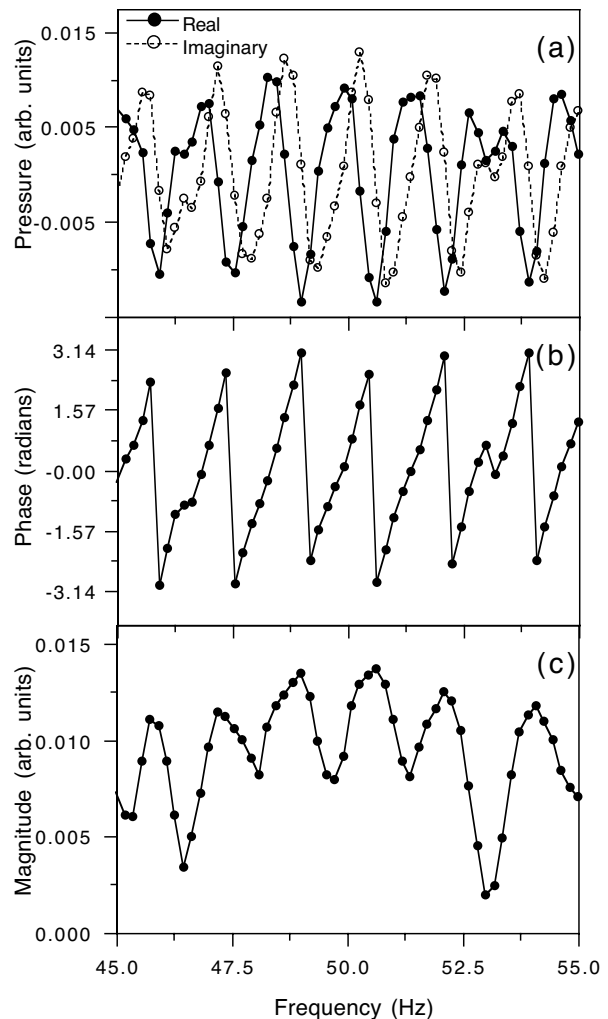


FIGURE 4 Complex field values for the example described in the text, (a) from NSPE, decomposed into (b) phase, and (c) magnitude components as a function of frequency at a receiver location. Circles indicate frequencies at which PE model was run. For clarity, only a small portion of the entire frequency range is shown. The actual frequency band spanned from 23 to 76 Hz, with zero padding out to 95 Hz. Note the wrapped linear behavior of the phase and the relatively smooth behavior of the magnitude, making both of these functions amenable to linear interpolation for intermediate values.

Example: In this case, an omnidirectional source emitting a Gaussian pulse 10 Hz wide centered on 50 Hz is used in a seamount environment with a sandy bottom. A field plot at the center frequency is shown in Fig. 5. The source is at 91 m depth, while the receiver is at 100 m on the right edge of the plot.

Time domain results are shown in Fig. 6 for (a) the real sound pressure and (b) the replica correlator output. The reference solution made with tight NSPE gridding and no frequency skipping is shown in blue, while the operational-grade solution is shown in black. Runtimes were 500.4 and 18.45 s, respectively, a 27-fold speed increase. Disabling the frequency skipping

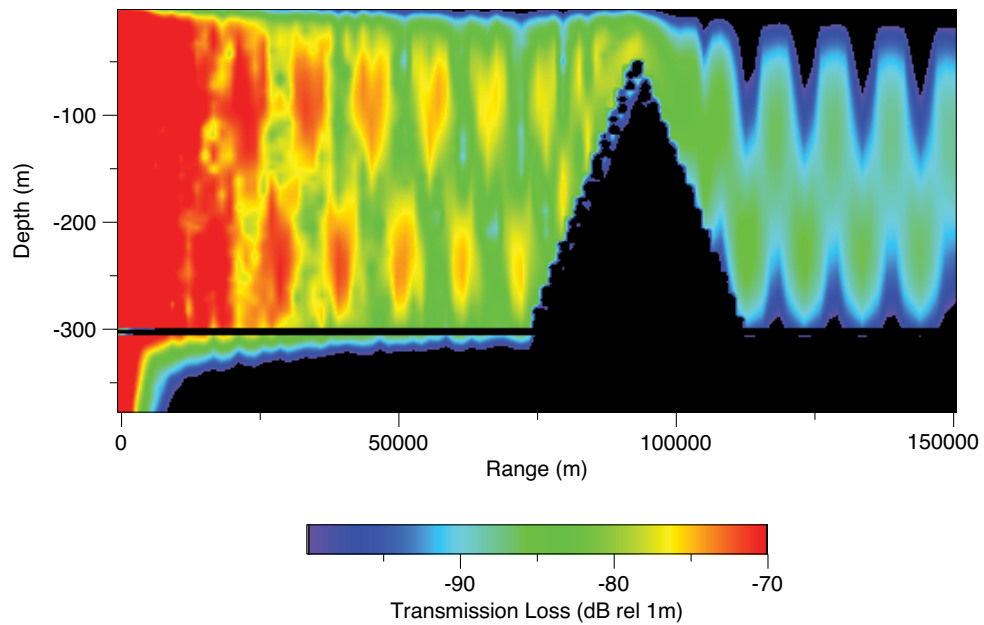


FIGURE 5 Full-field transmission loss plot at the Gaussian pulse center frequency for the example described in the text. A large seamant between 75 and 115 km is evident. The source location is at the left axis, at 91 m depth. The receiver is located on the right edge of the plot at 100 m depth.

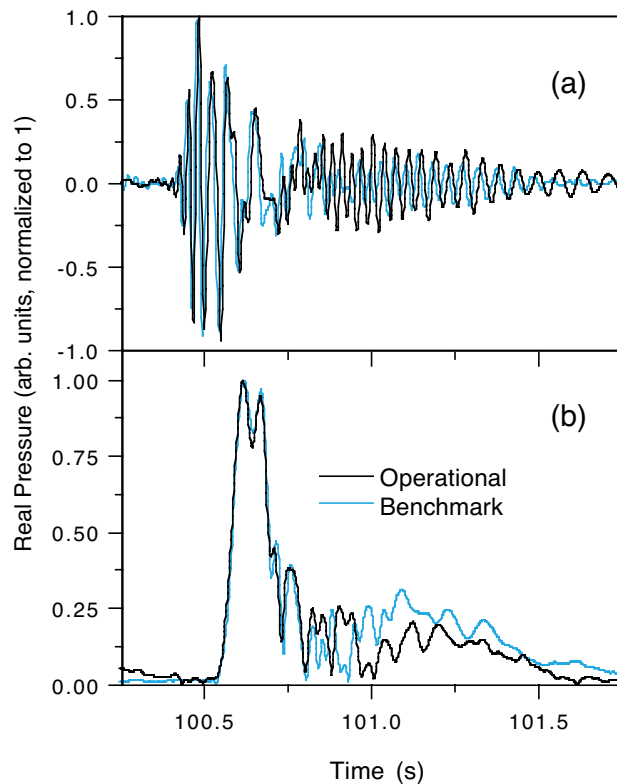


FIGURE 6 Time series results from the example described in the text, for the (a) real pressure and (b) replica correlator output. Results from operational grid and frequency interpolation settings are shown in black, while settings from research-grade settings are shown in cyan.

algorithm while retaining all other frequency-space optimizations and operational grid spacing gave a 45.86 s runtime, 2.5 times slower than the nonskipping version. For all PE grid settings and frequency skip factors used in these test runs, the pulse arrival times and transmission loss were in agreement at 100.6 s and 98 dB, respectively.

Summary: An algorithm to minimize the number of frequency-domain PE calculations required for Fourier synthesis of broadband time-domain pulses has been presented. An example in a challenging range-dependent seamount environment has been presented, with a 2.5-fold speedup over conventional optimizations demonstrated for full pulse waveform output, and a 24-fold speedup demonstrated when only arrival time and transmission loss are required. The software package is being readied for final delivery to the Navy for inclusion in the Ocean and Atmospheric Master Library.

[Sponsored by the NRL Base Program (CNR funded)]

References

- ¹R.A. Zingarelli, S.A. Chin-Bing, and M.D. Collins, "Optimizations for Fourier Synthesized Time Domain Pulse Propagation Calculations," Proceedings of the OCEANS 2009 MTS/IEEE Conference and Exhibition, Biloxi, MS, Oct. 26–29, 2009, pp. 2179–2183.
- ²R.A. Zingarelli and D.B. King, "RAM to Navy Standard Parabolic Equation: Transition from Research to Fleet Acoustic Model," 2003 NRL Review (Naval Research Laboratory, Washington, DC, 2003), pp. 212–214.
- ³W.H. Press et al., *Numerical Recipes, The Art of Scientific Computing (FORTRAN Version)* (Cambridge University Press, New York, 1989), pp. 381–429.



Range-Dependent Seismo-Acoustics

M.D. Collins
Acoustics Division

Introduction: Problems of interest in ocean acoustics typically involve grids that are much larger than a wavelength in both depth and range (horizontal distance), interaction with a seafloor that supports compressional (longitudinal) and shear (transverse) waves, and range dependence in the medium. It is usually not practical to directly solve the elliptic wave equation that governs such problems, which may often be solved routinely and accurately by reducing to a parabolic wave equation.¹ The key assumption in the derivation of a parabolic approximation is that outgoing energy dominates energy that is backscattered in the horizontal direction. In a stratified medium, arbitrarily accurate solutions may be obtained by using an appropriately

designed parabolic approximation. When the medium is range dependent, it is necessary to include a correction to guarantee that energy is conserved. This issue was unresolved for many years for the seismo-acoustic case involving a sloping fluid–solid interface at the seafloor. Appearing in Fig. 7 is a range-dependent problem involving an interface wave propagating along a sloping seafloor.

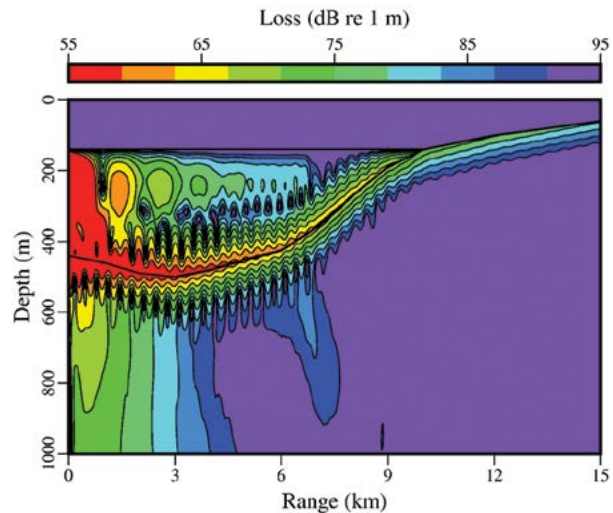


FIGURE 7

Seismo-acoustic propagation in an ocean environment with an upward sloping seafloor. A 5 Hz acoustic source is in the water column to the left, where the ocean depth is 320 m. After initially increasing, the ocean depth decreases all the way to the beach at a range of 10 km, and the slope continues beyond the shoreline. Energy concentrated near the seafloor corresponds to a Scholte wave, which becomes a Rayleigh wave beyond the shoreline. The ocean waveguide also supports a water-borne mode that transmits into the elastic sediment as a beam near a range of 7 km.

Single-Scattering Correction: The accuracy of the parabolic equation method was confirmed for range-independent acoustics problems in the late 1980s. Around the same time, it came to light that sloping interfaces and other types of range dependence may give rise to significant errors and even cause stability problems. In the implementations that were in use at the time, range dependence was handled with the naïve approach of approximating the medium in terms of a series of range-independent regions and conserving the dependent variable across the vertical interfaces between regions. For the purely acoustic case, effective corrections were developed within a few years using the concepts of energy conservation and single scattering. The seismic and seismo-acoustic cases proved to be much more challenging. A useful single-scattering correction was developed for the seismic case,² but it requires iterations that adversely affect efficiency and may not converge.

Improving the single-scattering correction for the seismic case so that iterations are no longer required led to a single-scattering correction for the seismo-acoustic case that has provided promising results.³ Since the elliptic wave equation has two range derivatives and the parabolic wave equation only has one range derivative, it is not possible to impose all of the conditions across vertical interfaces on solutions of the parabolic wave equation. For the acoustic case, effective results have been obtained by conserving quantities that guarantee that energy is conserved or to solve a single-scattering problem and discard the backscattered field (the latter approach may require iterations).

In the improved single-scattering solution for the seismic case, the transmitted field across a vertical interface consists of an average of two terms. One of the terms corresponds to conserving normal displacement and tangential stress. The other term corresponds to conserving tangential displacement and normal stress. The solution of the elliptic wave equation would be required to conserve all four quantities, but only two of them may be conserved in the solution of the parabolic wave equation. The improved single-scattering solution conserves these quantities in a mean sense; the transmitted field is the average of two fields that each correspond to conserving only two of the quantities. The simple physical interpretation of the improved single-scattering correction for the seismic case facilitated its extension to the seismo-acoustic case.³

Navy Standard Model: The earliest parabolic wave equations were based on crude approximations of the square root of a differential operator. The accuracy of this approach was suspect prior to the introduction of improved approximations based on rational functions. The next key step in the development of this approach was to incorporate the range numerics into the rational approximations; the parabolic wave equation is solved formally in terms of an exponential of the square root of an operator, which is then approximated in terms of a rational approximation.¹ This approach provides significant gains in efficiency and led to a major upgrade in the Navy Standard Model for ocean acoustic propagation. The Navy Standard Model does not currently account for shear waves, but it is anticipated that future versions will account for shear waves and handle them accurately using a single-scattering correction.

[Sponsored by the NRL Base Program (CNR funded)]

References

- ¹ M.D. Collins, "A Split-Step Padé Solution for the Parabolic Equation Method," *J. Acoust. Soc. Am.* **93**, 1736–1742 (1993).
- ² E.T. Küsel, W.L. Siegmann, and M.D. Collins, "A Single-Scattering Correction for Large Contrasts in Elastic Layers," *J. Acoust. Soc. Am.* **121**, 808–813 (2007).
- ³ M.D. Collins, "A Single-Scattering Correction for the Seismo-Acoustic Parabolic Equation," *J. Acoust. Soc. Am.* **131**, 2638–2642 (2012). ♦